Published in final edited form as:
Development. 2005 December ; 132(24): 5565–5575. doi:10.1242/dev.02155.

Normal myoblast fusion requires myoferlin

Katherine R. Doherty[1], **Andrew Cave**[2], **Dawn Belt Davis**[2], **Anthony J. Delmonte**[2], **Avery Posey**[2], **Judy U. Earley**[2], **Michele Hadhazy**[2], and **Elizabeth M. McNally**[2,3,*]

[1]Department of Molecular Genetics and Cell Biology, The University of Chicago, Chicago, IL 60637, USA

[2]Department of Medicine, The University of Chicago, Chicago, IL 60637, USA

[3]Department of Human Genetics, The University of Chicago, Chicago, IL 60637, USA

Summary

Muscle growth occurs during embryonic development and continues in adult life as regeneration. During embryonic muscle growth and regeneration in mature muscle, singly nucleated myoblasts fuse to each other to form myotubes. In muscle growth, singly nucleated myoblasts can also fuse to existing large, syncytial myofibers as a mechanism of increasing muscle mass without increasing myofiber number. Myoblast fusion requires the alignment and fusion of two apposed lipid bilayers. The repair of muscle plasma membrane disruptions also relies on the fusion of two apposed lipid bilayers. The protein dysferlin, the product of the Limb Girdle Muscular Dystrophy type 2 locus, has been shown to be necessary for efficient, calcium-sensitive, membrane resealing. We now show that the related protein myoferlin is highly expressed in myoblasts undergoing fusion, and is expressed at the site of myoblasts fusing to myotubes. Like dysferlin, we found that myoferlin binds phospholipids in a calcium-sensitive manner that requires the first C2A domain. We generated mice with a null allele of myoferlin. Myoferlin null myoblasts undergo initial fusion events, but they form large myotubes less efficiently in vitro, consistent with a defect in a later stage of myogenesis. In vivo, myoferlin null mice have smaller muscles than controls do, and myoferlin null muscle lacks large diameter myofibers. Additionally, myoferlin null muscle does not regenerate as well as wild-type muscle does, and instead displays a dystrophic phenotype. These data support a role for myoferlin in the maturation of myotubes and the formation of large myotubes that arise from the fusion of myoblasts to multinucleate myotubes.

Keywords

Myoblast; Fusion; Ferlin

Introduction

Muscle is composed of long, highly ordered, syncytial cells containing a near crystalline array of contractile proteins. Muscle develops from the initial fusion of singly nucleated myoblasts to each other to form myotubes. Myotube growth occurs through hypertrophy and

*Author for correspondence (emcnally@uchicago.edu).

the addition of singly nucleated myoblasts to the established syncytium. Two waves of myogenesis, termed primary and secondary myogenesis, are thought to occur in mammals (Ontell et al., 1988). By embryonic day 14, primary myofibers have formed in the mouse soleus muscle (Ontell et al., 1988). Between embryonic days 14–16, these primary myofibers grow through the fusion of new myoblasts with little de novo formation of myotubes (Ontell et al., 1988). Following this, a second wave of de novo myogenesis occurs, using the scaffold of myotubes formed during primary myogenesis. At birth, the soleus muscle contains the adult number of myofibers, and these fibers continue to grow through the fusion of myoblasts for at least the first five days of life (Ontell et al., 1988). Muscle is a regenerative organ, and parts of the myogenic process occur after muscle injury. Satellite cells are muscle precursor cells that after injury divide asymmetrically to maintain the satellite cell population and to create a pool of proliferating myoblasts (Mauro, 1961). These myoblasts may either fuse together forming de novo myofibers or fuse with existing myotubes in the injured muscle (Antonio and Gonyea, 1993; Kelley, 1996; Pena et al., 1995).

The genetic analysis of myogenesis in *Drosophila* has yielded considerable molecular information about the proteins mediating the attraction, adhesion and fusion of myoblasts (Chen and Olson, 2004). *Drosophila* myogenic cells are divided into founder cells and fusion-competent cells. Founder cells seed muscle development by attracting and fusing with fusion-competent cells to form small myotubes. Attraction and adhesion are mediated by the extracellular immunoglobulin domains in Dumbfounded (Duf; also known as Kirre, Kin of Irre) and Sticks and stones (Sns), which are expressed, respectively, on founder and fusion-competent cells (Bour et al., 2000; Ruiz-Gomez et al., 2000; Strunkelnberg et al., 2001). Mutations in the gene encoding myoblast city (Mbc), a protein that mediates cytoskeletal dynamics through Rac, produce a phenotype where fusion-competent cells adhere to founders, but fail to fuse (Erickson et al., 1997; Rushton et al., 1995). Rolling pebbles (Rols7; also know as Rols, or Antisocial or Ants), interacts with Mbc (Chen and Olson, 2001), and mutations in *Rols7* also affect fusion; some fusion-competent cells manage to fuse with founders, but these binucleate precursors fail to grow beyond this initial cellular fusion stage (Menon and Chia, 2001; Rau et al., 2001).

Differences exist between invertebrate and vertebrate myogenesis. Evidence for founder cells and fusion-competent cells in mammals is lacking. Based on sequence comparisons, the mammalian ortholog of *Duf* and *Sns* is nephrin, a gene involved in kidney development (Kestila et al., 1998; Lenkkeri et al., 1999). Mbc, and its vertebrate homolog DOCK180, are members of the CDM (CED-5, DOCK180, Myoblast city) family; members of this family have been classified as novel guanine nucleotide-exchange factors for Rho family GTPases, and they regulate diverse cellular pathways (Lu et al., 2005).

Despite the apparent lack of direct homology between *Drosophila* and mammalian myoblast fusion genes, some similar structural motifs are found. Like Duf and Sns, BOC and CDO are mammalian members of the immunoglobulin superfamily. Overexpression of either BOC or CDO enhances differentiation and fusion in the muscle cell line C2C12. The intracellular domain of CDO is thought to create a positive-feedback loop with MYOD and other myogenic transcription factors (Kang et al., 2002). CDO and BOC interact with N- and M-

cadherin in developing muscle cells (Cifuentes-Diaz et al., 1994; Hahn and Covault, 1992; Moore and Walsh, 1993; Rose et al., 1994). Interestingly, a CDO deletion mutant that cannot bind N-cadherin inhibits myoblast differentiation (Kang et al., 2003). M-cadherin is expressed in myoblasts and is further induced during differentiation (Donalies et al., 1991). In adult muscle, M-cadherin is expressed in satellite cells where it may function in regeneration (Bornemann and Schmalbruch, 1994; Irintchev et al., 1994). In the presence of peptides that block the self-interaction of M-cadherin, myoblasts do not fuse (Zeschnigk et al., 1995). Surface clustering of N-cadherins by ligand- or antibody-coated beads is sufficient to trigger fusion (Goichberg and Geiger, 1998). Activation of N-cadherin may be sufficient for differentiation, but it is not necessary, as myoblasts lacking N-cadherin fuse and differentiate normally (Charlton et al., 1997). These data suggest that there is functional redundancy among the cadherins during muscle development.

It is clear that the interactions of N- and M-cadherins with CDO and BOC play a role in differentiation, but the details of this process remain to be elucidated. In addition, experimental evidence implicates several transmembrane and membrane associated proteins such as ADAM12, β1 integrin, tetraspanin CD9, VLA4, VCAM1, caveolin 3 and calpain 3 in the myoblast fusion process (Horsley and Pavlath, 2004), but again the molecular mechanisms are not fully understood.

The mechanics of membrane fusion have been studied in other cell types. At nerve terminals, neurotransmitter release requires the regulation of synaptic vesicle fusion to the plasma membrane (Chapman, 2002). This fusion process relies on interactions among the SNARE proteins snytaxin, SNAP 25 and synaptobrevin to tether the vesicles to the plasma membrane. Upon increased intracellular calcium concentration, the C2A and C2B domains of synaptotagmin anchored in the vesicle, bind calcium and interact with SNARE proteins (Chapman et al., 1995; Davis et al., 1999; Shao et al., 1997). Synaptotagmin C2 domains are believed to insert into the plasma membrane phospholipids and trigger membrane fusion (Bai et al., 2002; Chapman and Davis, 1998; Chapman and Jahn, 1994), possibly by making fusion more energetically favorable (Chapman, 2002). The fusion of synaptic vesicles with the plasma membrane is calcium sensitive, and synaptotagmin has been proposed to be the calcium sensor (Brose et al., 1992; Fernandez-Chacon et al., 2001). Non-neuronal synaptotagmins regulate calcium-sensitive fusion of lysosomes with the plasma membrane to allow resealing after membrane disruptions in cells such as fibroblasts (Reddy et al., 2001).

Dysferlin has been implicated in vertebrate muscle membrane fusion. Dysferlin has structural and biochemical similarity to synaptotagmins, with six C2 domains and a carboxy-terminal transmembrane domain. The amino-terminal C2 domain, C2A, displays calcium-sensitive phospholipid binding in vitro (Davis et al., 2002). In addition, muscle fibers isolated from dysferlin null mice have markedly delayed membrane resealing even in the presence of calcium (Bansal et al., 2003; Lennon et al., 2003). This deficiency in cellular repair may underlie the muscular dystrophy phenotype seen in humans with dysferlin gene mutations (Bashir et al., 1998; Liu et al., 1998). Dysferlin-mediated muscular dystrophy is associated with the sub-plasmalemmal accumulation of vesicles (Cenacchi et al., 2005; Piccolo et al., 2000). A missense mutation in the C2A of dysferlin, V67D, is responsible for

muscular dystrophy (Illarioshkin et al., 2000), and abolishes C2A calcium-induced phospholipid binding in vitro (Davis et al., 2002).

Myoferlin is homologous to dysferlin and is expressed highly in developing muscle (Davis et al., 2000). We have now examined myoferlin expression in a cell-culture model of muscle differentiation, finding that it is expressed at the sites of apposed membranes undergoing fusion. We found that a mutation in myoferlin C2A disrupts calcium-induced phospholipid binding. We generated mice lacking myoferlin and found that myoferlin null myoblasts do not efficiently form large myotubes. Consistent with this, myoferlin null mice do not generate large myofibers. Finally, we studied muscle regeneration in myoferlin null mice and found that the later stages of muscle regeneration are defective. Our data indicate that myoferlin plays an important role in mediating myoblast fusion to myotubes during both development and muscle regeneration after injury.

Materials and methods

Antibodies, culture and imaging

C2C12 cells were obtained from ATCC (Catalog number CRL-1772). Cells were grown in DMEM supplemented with 10% fetal bovine serum and penicillin/streptomycin in 7% CO_2. Cells were induced to differentiate in DMEM with 2% horse serum.

For immunoblot analysis, C2C12 cells were plated at equal densities on 10 cm tissue culture plates and harvested at specified timepoints. 10^6 cells were lysed in 1 ml of lysis buffer [25 mM Tris (pH 7.4), 300 mM NaCl, 1 mM $CaCl_2$, 1% Triton-X 100 with Complete Mini Protease Inhibitor cocktail (Roche Molecular Biochemicals)]. Cellular debris was removed, and the protein concentration was determined using the Bio-Rad protein assay (Bio-Rad Protein Laboratories). 30 mg of protein was separated on a 4–10% acrylamide gel. Equivalently loaded gels were stained with Coomassie Blue or transferred to PVDF Immobilon-P membrane (Millipore).

Rabbit antiserum was raised to amino acids 1088–1107 of the mouse myoferlin protein (Proteintech Group, Chicago, IL). MYOF3 was antigen purified using the AminoLink Plus Immobilization Kit (Pierce). Purified antibody was concentrated in a YM-10 Centricon (Millipore). Polyclonal anti-myoferlin (MYOF3; 1:1000), monoclonal anti-dysferlin (1:1000, NCL-hamlet, Novocastra), monoclonal anti-annexin II antibody (1:5000, BD Biosciences) and anti-dystrophin 6–10 (1:15000) (Lidov et al., 1990) were used in 5% milk in 1×Tris-buffered saline with 0.1% Tween 20. Secondary antibodies, goat anti-mouse and goat anti-rabbit conjugated to horseradish peroxidase (Jackson ImmunoResearch) were used at a dilution of 1:5000. ECL-Plus chemiluminescence (Amersham-Pharmacia) and Kodak Biomax MS film or a Molecular Dynamics Phosphorimager was used for detection.

For immunofluorescence microscopy, cells were plated at equal densities in tissue culture plates containing glass coverslips. At specified timepoints, coverslips were fixed for 10 minutes in 4% paraformaldehyde in 1×PBS, then permeablized for 10 minutes in 0.3% Triton-X100. Coverslips were blocked in 1×PBS with 5% fetal bovine serum and 0.1% Triton-X 100, then incubated in this solution with MYOF3 and NCL-hamlet at a dilution of

1:100. A monoclonal anti-embryonic myosin heavy chain (eMyHC) F1.652 antibody (Developmental Studies Hybridoma Bank, University of Iowa) was used at a dilution of 1:5 and polyclonal anti-dystrophin 6–10 at a dilution of 1:200 in PBS containing 5% FBS and 0.1% Triton-X100. Monoclonal anti-caveolin 3 (BD Transduction Laboratories) was used at a dilution of 1:200. Goat anti-mouse conjugated to FITC, goat anti-rabbit conjugated to Cy3 (Jackson ImmunoResearch), goat anti-mouse conjugated to Alexa 488 or goat anti-rabbit conjugated to Alexa 594 (Molecular Probes) antibodies were used at a dilution of 1:2000 for detection. Coverslips were mounted using Vectashield with DAPI (Vector Laboratories), and images were captured using a Zeiss Axiophot microscope and Axiovision software (Carl Zeiss), or a Leica SP2 scanning laser confocal microscope and LCS Leica Confocal Software.

Calcium-dependent phospholipid binding

Calcium-dependent phospholipid binding was carried out as described (Davis et al., 2002). C2A domains were expressed as fusion proteins to glutathione S-transferase, bound to glutathione sepharose beads (Amersham Pharmacia Biotech), and incubated with tritiated-phosphotidyl liposomes composed of 50% phosphotidylcholine/50% phosphotidylserine in either calcium-free or 1 mM calcium buffer.

Generation of myoferlin null mice

The 1.7 kb short arm clone was amplified with a forward primer (BamHI/shortarm F CGGATCCCACCGAATGGCCTGACATTTCTGTA) that corresponded to the region 282 bp after the translational start site, and a reverse primer (KpnI/shortarm R ACGGTACCGCCATGGCTAAGGAAGCTGAGACCT) 1.7 kb downstream. This product was cloned into the *Bam*HI and *Kpn*I sites of the pPNT-loxP vector. The 9 kb clone for the long arm was amplified with a forward primer containing a *Not*I site (Long Arm NotI F AGAATGCGGCCGCGTACTGACTCCTTAAGTTGTCCCT) and a reverse primer in exon 1 (mMyo intronAR3 CCACACTCCCTCTCGGAGTCCACTC). The resulting product was digested with *Not*I and *Xho*I, and ligated to the pPNT vector that already contained the short arm. The transcriptional start site was predicted by Promoter Scan II (http://bimas.dcrt.nih.gov/molbio/proscan), and the transcription factor binding sites were predicted by TFSEARCH (http://molsun1.cbrc.aist.go.jp/research/db/TFSEARCH.html).

The targeting vector was linearized with *Not*I and electroporated into embryonic stem cells (Incyte). Three clones out of 117 were found to contain the predicted recombined allele. ES cells were injected into blastocysts and implanted into pseudopregnant females. Animals born from ES-injected blastocysts displayed chimerism in their coat color, ranging from 40–90%. As these mice produced a high percentage of germline offspring, we bred the high chimeric males to 129SV/J mice to produce mice on a 129SV/J background. Littermate control mice were used for comparison.

Isolation and culture of primary myoblasts

Primary myoblast cultures were isolated and cultured as described (Rando and Blau, 1994). For fusion assays, cells were counted after pre-plating, then plated in primary cell growth media [Ham's F-10 with 20% fetal bovine serum, and bFGF 2.5 ng/ml (Promega) with

antibiotic-antimycotic (Invitrogen 15240-062)] at 120,000 cells per well on ECL-treated plastic 4-well chamber slides (Lab-Tek, Nalge Nunc International). 6 hours later the media was changed (DMEM with 2% horse serum and PSA). 4 days after differentiation, cells were fixed for 2 minutes in methanol on ice, rehydrated in 1×PBS and blocked in 1×PBS with 5% fetal bovine serum and 0.1% Triton-X100. Cells were stained with monoclonal anti-desmin DE-U-10 (Sigma) at 1:300. They were then incubated with 0.05 μM Sytox Green nuclear stain (Molecular Probes) and goat anti-mouse Cy3 antibody. To quantify fusion, eight fields at 10× magnification were analyzed, using four fields from each of two separate cultures of each genotype. Using ImageJ, desmin-stained cells were classified as singly nucleated, containing 2–3 nuclei, or containing 4 or more nuclei (n=2390 wild-type and n=2485 myoferlin null nuclei). Statistical analysis was performed with InStat, using an unpaired t-test.

Analysis of cardiotoxin damage

Four-month-old wild-type and myoferlin null males were anaesthetized with isoflurane, and 100 μl of 10 μM cardiotoxin (CalBiochem) in 1×PBS was injected into the right gastrocnemius muscle. The animals were sacrificed by cervical dislocation at 3, 5, 7, 9, 11, 13 and 18 days after cardiotoxin injection. Gastrocnemii muscles were harvested tendon-to-tendon, mounted in OCT, fixed in chilled isopentane and frozen in liquid nitrogen. 10 μm sections were prepared on a cryostat, fixed in 10% formalin and stained with Masson's Trichrome. To quantify adipose and fibrotic infiltration, digital images were taken of injected muscle at days 9, 11 and 13 after injection. The blue fibrotic areas and white adipose infiltrates from four fields from the same region of the muscle at each time point from each genotype were measured using ImageJ. The areas infiltrated by fibrofatty replacement in wild-type and null muscle were compared by InStat, using an unpaired t-test with Welch correction. Sections from frozen gastrocnemii muscles were stained with Oil Red O stain and Mayer's Hematoxylin counterstain.

Muscle mass and fiber size analysis

The quadriceps, gastrocnemius/soleus, and triceps, were dissected free from tendon-to-tendon and weighed. Body and muscle masses were analyzed with InStat using an unpaired t-test with Welch correction. The quadriceps muscles were preserved in 10% formalin, bisected in the mid-belly and embedded in paraffin. Sections from the center of the muscle were stained with Masson Trichrome. Using ImageJ, the area of each fiber in three fields from each animal was determined using a total of 1740 wild-type and 2240 myoferlin null fibers. Average areas were compared using InStat and an unpaired t-test with Welch correction. ATPase staining was performed on 10 μm frozen muscle sections from four animals of each genotype at pH 4.6 and at pH 9.4 as described in http://www.neuro.wustl.edu/neuromuscular/pathol/histol/atp.htm.

Results

Myoferlin is expressed in myoblasts undergoing fusion to myotubes

C2C12 cells represent a cell-culture model of muscle differentiation (Yaffe and Saxel, 1977). The primary structure of dysferlin and myoferlin suggest a role in membrane fusion

processes, as these proteins include six C2 domains and a transmembrane domain (Fig. 1A). We examined the expression of dysferlin and myoferlin in C2C12 cells induced to undergo muscle differentiation by using antibodies specific for both myoferlin and dysferlin, MYOF3 and NCL-hamlet, respectively. We found that myoferlin expression is increased from its baseline in proliferating myoblasts (Fig. 1B, days 1 and 2), as well in differentiating myoblasts (Fig. 1B, days 3–8, the switch to differentiation media is indicated by the asterisk). By contrast, high levels of dysferlin do not appear until two days or more of differentiation (day 4). A small amount of dysferlin is visible at earlier time points by immunoblotting because the differentiation of these cultures is not perfectly synchronized. As these cultures represent a mix of cells at different stages of maturation, we performed immunofluorescence microscopy at the same timepoints as in Fig. 1B to further characterize the timing of ferlin expression in C2C12 cell culture. We found that there is little overlap in the expression of the two proteins (very little yellow is visible in the merged images in Fig. 1C). Myoferlin was expressed highly in undifferentiated and early differentiating single-nucleated myoblasts (Fig. 1C, days 1 and 3). At day 3, dysferlin expression was detected, but only in multinucleate myotubes. In cultures containing both singly nucleated myoblasts and multinucleated myotubes, myoferlin expression was greater in myoblasts (Fig. 1C, days 4 and 6). Dysferlin immunoreactivity appeared in a punctate pattern along the myotube membrane, which is consistent with a potential localization in subplasmalemmal vesicles (Bansal et al., 2003) (data not shown).

Because myoferlin was highly expressed at the stage in which myoblasts are undergoing fusion, we examined myoferlin expression in primary cultured myoblasts using confocal microscopy. Myoferlin was found to be highly concentrated at the site of apposed myoblast and myotube membranes (Fig. 2A, arrow). Myoferlin was also concentrated at sites of contact between two myotubes (Fig. 2A,B), and these areas colocalized with caveolin 3, a membrane-associated protein (Fig. 2B). In addition to being concentrated at sites of myoblast fusion, myoferlin displayed biochemical properties consistent with a role in membrane fusion. Bacterially expressed and purified myoferlin C2A bound to vesicles containing 50% phosphotidylserine/50% phosphotidylcholine in a calcium-dependent manner that was consistent with our previously published findings (Davis et al., 2002). A point mutation, I67D, was engineered into the myoferlin C2A domain. In dysferlin, the homologous mutation (V67D) results in muscular dystrophy in humans (Illarioshkin et al., 2000), and reduces calcium-sensitive phospholipid binding in vitro (Davis et al., 2002). A similar point mutation, I67D, in myoferlin C2A also completely abolishes calcium-sensitive phospholipid binding (Fig. 2C). Half-maximal phospholipid binding of myoferlin C2A occurs at 1 μM calcium, which is similar to the 1.4 μM calcium concentration reported in fusing myoblasts (Przybylski et al., 1994).

Myoferlin null myoblasts do not fuse efficiently

To further understand the in vivo role of myoferlin, we generated myoferlin null mice. The myoferlin (fer1L3) locus is 52 exons over 144.5 kilobases of chromosome 19 (Fig. 3A). As shown in Fig. 3, homologous recombination resulted in the deletion of exon 1 containing the 5′ untranslated region, the initiation codon and the transcriptional start site. Transcripts starting at exon 2 were detectable by RT-PCR (data not shown), but protein correlating to

these transcripts was not detected. Translation of this mRNA would produce a protein of approximately 210 kDa lacking the C2A domain. To verify the absence of myoferlin production from the null allele, myoblasts were isolated from myoferlin null and littermate mice, cultured, differentiated for five days, and assessed by confocal immunofluorescence microscopy (Fig. 3D) and immunoblotting (Fig. 3E). Neither full-length nor truncated myoferlin proteins were detected. Consistent with the loss of myoferlin and compensation by the related protein, an increase in dysferlin protein expression was detected in cultured myotubes. The expression of other muscle membrane-associated proteins, such as dystrophin and annexin II, was not altered in myoferlin null myoblasts. To further investigate the upregulation of dysferlin, quantitative immunoblotting was used on wild-type and myoferlin null myoblast/myotube cultures at various timepoints. Wild-type and myoferlin null cultures of confluent myoblasts and cells that had been exposed to differentiation media for 24 hours expressed equivalent levels of dysferlin (data not shown). After 4 days of differentiation, dysferlin expression was 1.6-fold higher in myoferlin null cultures than in wild type.

The fusion properties of myoblast cultures from myoferlin null and littermate control neonatal mice were compared. Fusion indices were determined for myoferlin and littermate cultures by using desmin immunoreactivity to identify singly nucleated myoblasts and myotubes (red in Fig. 4A). Wild-type and myoferlin null cells were plated in equal numbers at high density in chamber slides. Six hours later, growth media was replaced with differentiation media to ensure that any proliferative difference would not affect cell density, and, subsequently, cell fusion. After 4 days in differentiation media, the slides were fixed and stained for desmin. Eight fields of each genotype were photographed at 10× magnification, and each nucleus in a desmin-positive cell was marked as being in a singly nucleated myoblast (white square), in a myotube containing two or three nuclei (green square), or in a myotube containing four or more nuclei (blue square), as shown in the illustrative examples in Fig. 4A. Myoferlin null cultures were noted to have significantly more singly nucleated desmin-positive cells than wild-type cultures had. Small myotubes, those containing two to three nuclei, were not significantly different in myoferlin null and control cultures. Myoferlin null myoblast cultures displayed fewer large multinucleated myotubes, designated as those myotubes with greater than four nuclei (Fig. 4). The fusion index, defined as the percentage of nuclei in myotubes containing five or more nuclei, was 59% for wild-type and 41% for myoferlin null cultures after four days of differentiation (P=0.002). These findings confirm that singly nucleated myoferlin null myoblasts are impaired in their ability to form larger myotubes.

Myoferlin null mice have smaller muscles with few large fibers

The loss of myoferlin had no detrimental effect on viability, fertility or longevity up to 12 months of age. However, myoferlin null mice were significantly smaller than their littermate controls (Fig. 5A). Individual muscle groups were examined revealing that muscles from myoferlin mice were smaller than those of littermate controls (n=7, null; n=6, wildtype) (Fig. 5B). Myoferlin null muscles have smaller myofibers (Fig. 5C). Mean fiber size was significantly smaller in myoferlin null muscle than in littermate controls (Fig. 5D). The median wild-type fiber size was 2,205 μm^2, whereas the myoferlin null median was 1,711

μm^2. The distribution of fiber size showed an overrepresentation of smaller myofibers in myoferlin null muscle (Fig. 5E, red). Larger myofibers were lacking in myoferlin null muscle. Myofibers with an area of greater than 4,300 μm^2 make up 7.4% of wild type fibers; fibers this size are markedly reduced in myoferlin null quadriceps muscle, making up only 0.33% of the total.

Fiber size was also analyzed in muscles from the upper limb of neonatal mice, as myoferlin is expressed during embryogenesis (Davis et al., 2000) and its absence could have a phenotypic effect earlier in development. At this age, there was no difference in average fiber area between wild-type (n=3) and myoferlin null (n=3) muscle (159 μm^2 and 155 μm^2, respectively; P=0.5). The median fiber area for the myoferlin null muscles (131 μm^2) was smaller than that of the wild type (148 μm^2), indicating that the distribution of fiber size was shifted in myoferlin null mice at this stage of development, although not nearly as much as in adults animals. These data support a role for myoferlin in normal muscle growth, and, specifically, in the growth of large myofibers that appear later during muscle maturation.

We further examined fiber type distribution in myoferlin null muscles. At four months of age, the fiber distribution of the gastrocnemius was equivalent in wild-type (61% type IIA and 39% type IIB) and in myoferlin null (58% type IIA and 42% type IIB) animals (P=0.48). As in normal muscle, no type I fibers were detected in the quadriceps, triceps or gastrocnemii of myoferlin null mice. The soleus of myoferlin null mice contained significantly more type I fibers than did the wild type (50% compared with 37%, respectively; P=0.008). At one month of age, this difference was more pronounced. The myoferlin null soleus was made up of 51% type I, whereas wild type contained only 18.5% type I fibers (P=0.0001). This suggests that the growth of type II fibers may be more affected by the loss of myoferlin.

Myoferlin null mice fail to fully regenerate muscle after injury

Myoblast fusion also plays a vital role in healing and regenerating muscle after injury. To determine what role myoferlin might play in this fusion process, cardiotoxin was injected into the gastrocnemius of wild-type and myoferlin mice (d'Albis et al., 1989; Davis et al., 1993). Cardiotoxins are polypeptides of 60–65 amino acids isolated from cobra venom, and cause depolarization and degradation of the plasma membrane. This degeneration activates satellite cells to proliferate and fuse to form new myofibers (Snow, 1977). From 1–3 days post-injection, the site of injury consists of a mononuclear infiltrate composed of inflammatory cells and activated myoblasts. By day 5, centrally nucleated fibers, indicative of regeneration, are visible. New fibers continue to form and grow through fusion events, and at 30 days, although muscle architecture has been fully restored, many centrally placed nuclei may remain (Kherif et al., 1999).

The levels of myoferlin protein were examined 5 days after cardiotoxin injection. The entire gastrocnemius muscle was dissected tendon-to-tendon and homogenized. Immunoblotting showed that myoferlin was present at low levels in wild-type muscle, and that it is very strongly induced 5 days after cardiotoxin injection (Fig. 6A, lanes 1 and 3). Dysferlin was present at equal levels in both injured and control muscle of wild-type and myoferlin null

mice. After injury, high levels of myoferlin are expressed in a diffuse pattern in areas of mononuclear infiltration and regeneration (data not shown).

Cardiotoxin injections were performed in myoferlin null and control gastrocnemii muscle. At day 11 after cardiotoxin injection (Fig. 6B), both wild-type and myoferlin null muscle show scattered fibers expressing embryonic myosin-positive fibers (red) consistent with regeneration. Dystrophin staining shows that myoferlin null muscle contains irregularly shaped fibers with a greater fiber size distribution than control muscle. The large dystrophin-negative cells seen in the myoferlin null images represent degenerating fibers. By comparison, at 11 days after cardiotoxin injection, the wild-type muscle exhibits fewer of these fibers and has regained a normal overall architecture similar to uninjured muscle with smoothly outlined myofibers,

Overall, myoferlin null muscle displayed a slower and more incomplete regenerative response than wild-type muscle did. Both wild-type and myoferlin null muscles showed mononuclear infiltrates 3 days after injection, and small, centrally nucleated fibers indicative of regeneration at 5 days (data not shown). 9, 11 and 13 days after cardiotoxin injection, approximately midway through the regenerative process, Masson trichrome staining showed evidence of the replacement of muscle with fibrotic connective tissue (arrow in Fig. 7A) and adipose cell infiltrates (arrowheads in Fig. 7A) in myoferlin null muscle. Oil Red O, a lipid specific dye (Fig. 7B), showed larger and more numerous fat-containing cells. Fibrofatty replacement was additionally evaluated. Myoferlin null gastrocnemius muscles had significantly more fibrous and fatty infiltration after cardiotoxin-induced damage than did wild-type muscles (Fig. 7C). These data support a role for myoferlin specifically in the growth of large myofibers during development and regeneration.

Discussion

Myoferlin mediates myoblast fusion

We found that myoferlin is expressed in cultured myoblasts just prior to and during fusion events, and that myoferlin is concentrated at the membrane at sites of cell-cell contact. Through its C2A domain, myoferlin bound phospholipids in response to increased calcium concentration. In vivo, myoferlin null mice displayed an abnormal skeletal muscle phenotype, which is predicted to result from a failure of myofibers to grow efficiently through additional myoblast fusion. The area of individual muscle fibers was significantly reduced in these animals, leading to a reduction in cross-sectional area of whole muscle, and a significant decrease in muscle mass. Myoblasts cultured from myoferlin null mice showed a similar fusion defect, where the formation of larger myotubes in culture was less efficient. Mice lacking myoferlin are also impaired in their ability to regenerate skeletal muscle after injury. Normally, this process recapitulates the developmental process, with the de novo formation of myofibers that grow through fusion to replace fibers lost to damage, and myoferlin is upregulated in this process. Myoferlin null mice showed incomplete regeneration after injury, with disorganized muscle architecture with fibro-fatty infiltration rather than new myofibers.

Vertebrate myoblast fusion occurs as at least two different processes. We propose to refer to the process of the initial fusion of myoblasts to each other as `myoinitiation'. Myoinitiation occurs during muscle development and may also occur during the muscle regeneration that occurs in response to muscle injury. A second process, that is molecularly distinct from the first, is the process whereby myoblasts fuse to existing myotubes. We propose to refer to this process as `myoaugmentation'. The cytoskeletal rearrangements that must occur within myotubes to accommodate fusing myoblasts are not understood, but must differ from what occurs with myoblasts, given the existing sarcomeric structure present in myotubes. The phenotype of myoferlin null mice is reminiscent of *Drosophila* mutants in which bi- and trinucleated muscle precursors form, but fail to grow by recruiting fusion-competent cells (Menon and Chia, 2001; Rau et al., 2001; Schroter et al., 2004). Indeed, several different genetic mutants in *Drosophila* myogenesis support two distinct mechanisms akin to myoinitiation and myoaugmentation. Mutants that specifically affect the later process of myoaugmentation are seen in the form of mutations in the genes *rolling pebbles* (*rols*)/ *antisocial* (*ants*), as these mutants produce an accumulation of bi- or tri-nucleated muscle precursor cells (Chen and Olson, 2001). Rols/Ants is thought to be a cytoskeletal adaptor, further highlighting the importance of cytoskeletal rearrangements in this process. Additionally, mutations in the genes *kette* and *blown fuse*, which are also thought to affect the myoaugmentation process, are thought to affect the actin cytoskeleton (Schroter et al., 2004). Myoferlin is a protein that associates with the plasma membrane at the sites of both myoblast-myoblast fusion and myoblast-myotube fusion. However, myoferlin null mice appear to be less efficient in myoblast-myotube fusion. We hypothesize that myoferlin, through calcium-sensitive phospholipid binding, is more important for myoblast-myotube fusion or myoaugmentation. Myoferlin and dysferlin have no clear homologs in *Drosophila*. This may be because the primary functions of these ferlins seem to involve the repair and regeneration of large myotubes, and these processes are absent in flies.

Redundancy of ferlin proteins for fusion

The loss of myoferlin does not completely block the process of myogenesis, but rather renders it less efficient. This could be because dysferlin, or other uncharacterized members of the ferlin family (*fer1L4* and *fer1L5*), are able to partially compensate for the loss of myoferlin. In primary myoblast cultures, dysferlin is expressed at higher levels in myoferlin null cells than in wild-type cells, suggesting that it can at least partially compensate for the absence of myoferlin. Dysferlin does not appear to be upregulated in adult muscle in the absence of myoferlin. This may be due to the fact that myoferlin is present at such low levels in healthy adult muscle (Fig. 6A). There may be some upregulation of dysferlin in response to damage in myoferlin null mice (data not shown). The fact that we do not detect upregulation of dysferlin in myoferlin null myoblasts until later in the fusion process (Fig. 3E), when most of the fusion events involve fusion to large myotubes, supports the hypothesis that myoferlin is more important for mediating the fusion of myoblasts to myotubes, rather than between myoblasts. The biochemical properties of dysferlin and myoferlin differ, as the C2A domain of dysferlin displays a different sensitivity, showing half-maximal phospholipid binding at 4.5 μm rather than 1 μm calcium (Davis et al., 2002). This difference could also account for the impaired myoblast fusion seen in myoferlin null cells, in that increased dysferlin levels may be less effective at mediating membrane fusion.

Mechanisms of membrane fusion

Recent work on dysferlin null myotubes indicates that they are deficient in calcium-dependent membrane repair (Bansal et al., 2003; Lennon et al., 2003). In addition, electron micrographs of muscles from patients (Cenacchi et al., 2005; Piccolo et al., 2000) and mice (Bansal et al., 2003; Ho et al., 2004) show an accumulation of vesicles at the sarcolemma. On the basis of these data, models have been proposed in which dysferlin, anchored by its transmembrane domain either in the sarcolemmal membrane (Lennon et al., 2003) or in the repair vesicles (Bansal et al., 2003), or in a combination of both topologies (Doherty and McNally, 2003), serves to recruit vesicles to the site of membrane disruption to generate a patch. Interestingly, in electron micrographs, intracellular vesicles are seen at sites of membrane contact during fusion in cultured chick myoblasts (Kalderon and Gilula, 1979), and in *Drosophila* embryos (Doberstein et al., 1997). In *Drosophila* myoblasts, the vesicles are juxtaposed within each of the apposed cells at high density to create electron-dense areas of membrane. Following the appearance of the electron-dense area, there is dissolution and vesiculation of the dual plasma membrane region, resulting in a contiguous single membrane and continuity with the cytoplasm of the apposing cell (Doberstein et al., 1997). The initial alignment of vesicles across the electron-dense, dual plasma membrane is thought to be highly critical. *Drosophila mbc* mutants show neither vesicle alignment nor an electron-dense membrane, and, in this model, myoblasts completely fail to fuse (Doberstein et al., 1997).

The primary structure and biochemical properties of myoferlin and dysferlin suggest that these ferlins may act as calcium sensors. The process for membrane resealing and the process of myoblast fusion may both use specialized vesicles, and the ferlins may regulate the calcium sensitivity of vesicular fusion. The membrane-associated nature of ferlin proteins, along with the additional C2 domains, may serve to act as a scaffold for other proteins that are important for fusion processes; these proteins remain to be discovered. Dysferlin has been shown to interact with annexins A1 and A2 in a manner that changes with membrane disruption (Lennon et al., 2003). We have not detected a similar interaction for myoferlin with annexins (data not shown), but this may highlight molecular differences between sarcolemmal resealing and myoblast fusion. The coordinate expression of myoferlin and dysferlin in myoblasts and myotubes, respectively, supports an overlapping yet specialized role for these proteins in membrane fusion events.

Acknowledgments

This work was supported by the NIH-NINDS, the Muscular Dystrophy Association and a Burroughs Wellcome Award (E.M.M.). K.R.D. was supported by the NSF and the NIH.

References

Antonio J, Gonyea WJ. Skeletal muscle fiber hyperplasia. Med. Sci. Sports Exerc. 1993; 25:1333–1345. [PubMed: 8107539]

Bai J, Wang P, Chapman ER. C2A activates a cryptic Ca(2+)-triggered membrane penetration activity within the C2B domain of synaptotagmin I. Proc. Natl. Acad. Sci. USA. 2002; 99:1665–1670. [PubMed: 11805296]

Bansal D, Miyake K, Vogel SS, Groh S, Chen CC, Williamson R, McNeil PL, Campbell KP. Defective membrane repair in dysferlin-deficient muscular dystrophy. Nature. 2003; 423:168–172. [PubMed: 12736685]

Bashir R, Britton S, Strachan T, Keers S, Vafiadaki E, Lako M, Richard I, Marchand S, Bourg N, Argov Z, et al. A gene related to Caenorhabditis elegans spermatogenesis factor fer-1 is mutated in limb-girdle muscular dystrophy type 2B. Nat. Genet. 1998; 20:37–42. [PubMed: 9731527]

Bornemann A, Schmalbruch H. Immunocytochemistry of M-cadherin in mature and regenerating rat muscle. Anat. Rec. 1994; 239:119–125. [PubMed: 8059975]

Bour BA, Chakravarti M, West JM, Abmayr SM. Drosophila SNS, a member of the immunoglobulin superfamily that is essential for myoblast fusion. Genes Dev. 2000; 14:1498–1511. [PubMed: 10859168]

Brose N, Petrenko AG, Sudhof TC, Jahn R. Synaptotagmin: a calcium sensor on the synaptic vesicle surface. Science. 1992; 256:1021–1025. [PubMed: 1589771]

Cenacchi G, Fanin M, De Giorgi LB, Angelini C. Ultrastructural changes in dysferlinopathy support defective membrane repair mechanism. J. Clin. Pathol. 2005; 58:190–195. [PubMed: 15677541]

Chapman ER. Synaptotagmin: a Ca(2+) sensor that triggers exocytosis? Nat. Rev. Mol. Cell. Biol. 2002; 3:498–508. [PubMed: 12094216]

Chapman ER, Jahn R. Calcium-dependent interaction of the cytoplasmic region of synaptotagmin with membranes. Autonomous function of a single C2-homologous domain. J. Biol. Chem. 1994; 269:5735–5741. [PubMed: 8119912]

Chapman ER, Davis AF. Direct interaction of a Ca2+-binding loop of synaptotagmin with lipid bilayers. J. Biol. Chem. 1998; 273:13995–14001. [PubMed: 9593749]

Chapman ER, Hanson PI, An S, Jahn R. Ca2+ regulates the interaction between synaptotagmin and syntaxin 1. J. Biol. Chem. 1995; 270:23667–23671. [PubMed: 7559535]

Charlton CA, Mohler WA, Radice GL, Hynes RO, Blau HM. Fusion competence of myoblasts rendered genetically null for N-cadherin in culture. J. Cell Biol. 1997; 138:331–336. [PubMed: 9230075]

Chen EH, Olson EN. Antisocial, an intracellular adaptor protein, is required for myoblast fusion in Drosophila. Dev. Cell. 2001; 1:705–715. [PubMed: 11709190]

Chen EH, Olson EN. Towards a molecular pathway for myoblast fusion in Drosophila. Trends Cell Biol. 2004; 14:452–460. [PubMed: 15308212]

Cifuentes-Diaz C, Nicolet M, Goudou D, Rieger F, Mege RM. N-cadherin expression in developing, adult and denervated chicken neuromuscular system: accumulations at both the neuromuscular junction and the node of Ranvier. Development. 1994; 120:1–11. [PubMed: 8119118]

d'Albis A, Couteaux R, Janmot C, Mira JC. Myosin isoform transitions in regeneration of fast and slow muscles during postnatal development of the rat. Dev. Biol. 1989; 135:320–325. [PubMed: 2776971]

Davis AF, Bai J, Fasshauer D, Wolowick MJ, Lewis JL, Chapman ER. Kinetics of synaptotagmin responses to Ca2+ and assembly with the core SNARE complex onto membranes. Neuron. 1999; 24:363–376. [PubMed: 10571230]

Davis DB, Delmonte AJ, Ly CT, McNally EM. Myoferlin, a candidate gene and potential modifier of muscular dystrophy. Hum. Mol. Genet. 2000; 9:217–226. [PubMed: 10607832]

Davis DB, Doherty KR, Delmonte AJ, McNally EM. Calcium-sensitive phospholipid binding properties of normal and mutant ferlin C2 domains. J. Biol. Chem. 2002; 277:22883–22888. [PubMed: 11959863]

Davis HL, Demeneix BA, Quantin B, Coulombe J, Whalen RG. Plasmid DNA is superior to viral vectors for direct gene transfer into adult mouse skeletal muscle. Hum. Gene Ther. 1993; 4:733–740. [PubMed: 8186288]

Doberstein SK, Fetter RD, Mehta AY, Goodman CS. Genetic analysis of myoblast fusion: blown fuse is required for progression beyond the prefusion complex. J. Cell Biol. 1997; 136:1249–1261. [PubMed: 9087441]

Doherty KR, McNally EM. Repairing the tears: dysferlin in muscle membrane repair. Trends Mol. Med. 2003; 9:327–330. [PubMed: 12928033]

Donalies M, Cramer M, Ringwald M, Starzinski-Powitz A. Expression of M-cadherin, a member of the cadherin multigene family, correlates with differentiation of skeletal muscle cells. Proc. Natl. Acad. Sci. USA. 1991; 88:8024–8028. [PubMed: 1840697]

Erickson MR, Galletta BJ, Abmayr SM. Drosophila myoblast city encodes a conserved protein that is essential for myoblast fusion, dorsal closure, and cytoskeletal organization. J. Cell Biol. 1997; 138:589–603. [PubMed: 9245788]

Fernandez-Chacon R, Konigstorfer A, Gerber SH, Garcia J, Matos MF, Stevens CF, Brose N, Rizo J, Rosenmund C, Sudhof TC. Synaptotagmin I functions as a calcium regulator of release probability. Nature. 2001; 410:41–49. [PubMed: 11242035]

Goichberg P, Geiger B. Direct involvement of N-cadherin-mediated signaling in muscle differentiation. Mol. Biol. Cell. 1998; 9:3119–3131. [PubMed: 9802901]

Hahn CG, Covault J. Neural regulation of N-cadherin gene expression in developing and adult skeletal muscle. J. Neurosci. 1992; 12:4677–4687. [PubMed: 1464762]

Ho M, Post CM, Donahue LR, Lidov HG, Bronson RT, Goolsby H, Watkins SC, Cox GA, Brown RH Jr. Disruption of muscle membrane and phenotype divergence in two novel mouse models of dysferlin deficiency. Hum. Mol. Genet. 2004; 13:1999–2010. [PubMed: 15254015]

Horsley V, Pavlath GK. Forming a multinucleated cell: molecules that regulate myoblast fusion. Cells Tissues Organs. 2004; 176:67–78. [PubMed: 14745236]

Illarioshkin SN, Ivanova-Smolenskaya IA, Greenberg CR, Nylen E, Sukhorukov VS, Poleshchuk VV, Markova ED, Wrogemann K. Identical dysferlin mutation in limb-girdle muscular dystrophy type 2B and distal myopathy. Neurology. 2000; 55:1931–1933. [PubMed: 11134403]

Irintchev A, Zeschnigk M, Starzinski-Powitz A, Wernig A. Expression pattern of M-cadherin in normal, denervated, and regenerating mouse muscles. Dev. Dyn. 1994; 199:326–337. [PubMed: 8075434]

Kalderon N, Gilula NB. Membrane events involved in myoblast fusion. J. Cell Biol. 1979; 81:411–425. [PubMed: 468911]

Kang JS, Mulieri PJ, Hu Y, Taliana L, Krauss RS. BOC, an Ig superfamily member, associates with CDO to positively regulate myogenic differentiation. EMBO J. 2002; 21:114–124. [PubMed: 11782431]

Kang JS, Feinleib JL, Knox S, Ketteringham MA, Krauss RS. Promyogenic members of the Ig and cadherin families associate to positively regulate differentiation. Proc. Natl. Acad. Sci. USA. 2003; 100:3989–3994. [PubMed: 12634428]

Kelley G. Mechanical overload and skeletal muscle fiber hyperplasia: a meta-analysis. J. Appl. Physiol. 1996; 81:1584–1588. [PubMed: 8904572]

Kestila M, Lenkkeri U, Mannikko M, Lamerdin J, McCready P, Putaala H, Ruotsalainen V, Morita T, Nissinen M, Herva R, et al. Positionally cloned gene for a novel glomerular protein–nephrin–is mutated in congenital nephrotic syndrome. Mol. Cell. 1998; 1:575–582. [PubMed: 9660941]

Kherif S, Lafuma C, Dehaupas M, Lachkar S, Fournier JG, Verdiere-Sahuque M, Fardeau M, Alameddine HS. Expression of matrix metalloproteinases 2 and 9 in regenerating skeletal muscle: a study in experimentally injured and mdx muscles. Dev. Biol. 1999; 205:158–170. [PubMed: 9882504]

Lenkkeri U, Mannikko M, McCready P, Lamerdin J, Gribouval O, Niaudet PM, Antignac CK, Kashtan CE, Homberg C, Olsen A, et al. Structure of the gene for congenital nephrotic syndrome of the finnish type (NPHS1) and characterization of mutations. Am. J. Hum. Genet. 1999; 64:51–61. [PubMed: 9915943]

Lennon NJ, Kho A, Bacskai BJ, Perlmutter SL, Hyman BT, Brown RH Jr. Dysferlin interacts with annexins A1 and A2 and mediates sarcolemmal wound-healing. J. Biol. Chem. 2003; 278:50466–50473. [PubMed: 14506282]

Lidov HG, Byers TJ, Watkins SC, Kunkel LM. Localization of dystrophin to postsynaptic regions of central nervous system cortical neurons. Nature. 1990; 348:725–728. [PubMed: 2259381]

Liu J, Aoki M, Illa I, Wu C, Fardeau M, Angelini C, Serrano C, Urtizberea JA, Hentati F, Hamida MB, et al. Dysferlin, a novel skeletal muscle gene, is mutated in Miyoshi myopathy and limb girdle muscular dystrophy. Nat. Genet. 1998; 20:31–36. [PubMed: 9731526]

Lu M, Kinchen JM, Rossman KL, Grimsley C, Hall M, Sondek J, Hengartner MO, Yajnik V, Ravichandran KS. A Steric-inhibition model for regulation of nucleotide exchange via the Dock180 family of GEFs. Curr. Biol. 2005; 15:371–377. [PubMed: 15723800]

Mauro A. Satellite cell of skeletal muscle fibers. J. Biophys. Biochem. Cytol. 1961; 9:493–495. [PubMed: 13768451]

Menon SD, Chia W. Drosophila rolling pebbles: a multidomain protein required for myoblast fusion that recruits D-Titin in response to the myoblast attractant Dumbfounded. Dev. Cell. 2001; 1:691–703. [PubMed: 11709189]

Moore R, Walsh FS. The cell adhesion molecule M-cadherin is specifically expressed in developing and regenerating, but not denervated skeletal muscle. Development. 1993; 117:1409–1420. [PubMed: 8404540]

Ontell M, Hughes D, Bourke D. Morphometric analysis of the developing mouse soleus muscle. Am. J. Anat. 1988; 181:279–288. [PubMed: 3364386]

Pena J, Jimena I, Luque E, Vaamonde R. New fiber formation in rat soleus muscle following administration of denervated muscle extract. J. Neurol. Sci. 1995; 128:14–21. [PubMed: 7722530]

Piccolo F, Moore SA, Ford GC, Campbell KP. Intracellular accumulation and reduced sarcolemmal expression of dysferlin in limb–girdle muscular dystrophies. Ann. Neurol. 2000; 48:902–912. [PubMed: 11117547]

Przybylski RJ, Szigeti V, Davidheiser S, Kirby AC. Calcium regulation of skeletal myogenesis. II. Extracellular and cell surface effects. Cell Calcium. 1994; 15:132–142. [PubMed: 8149413]

Rando TA, Blau HM. Primary mouse myoblast purification, characterization, and transplantation for cell-mediated gene therapy. J. Cell Biol. 1994; 125:1275–1287. [PubMed: 8207057]

Rau A, Buttgereit D, Holz A, Fetter R, Doberstein SK, Paululat A, Staudt N, Skeath J, Michelson AM, Renkawitz-Pohl R. rolling pebbles (rols) is required in Drosophila muscle precursors for recruitment of myoblasts for fusion. Development. 2001; 128:5061–5073. [PubMed: 11748142]

Reddy A, Caler EV, Andrews NW. Plasma membrane repair is mediated by Ca(2+)-regulated exocytosis of lysosomes. Cell. 2001; 106:157–169. [PubMed: 11511344]

Rose O, Rohwedel J, Reinhardt S, Bachmann M, Cramer M, Rotter M, Wobus A, Starzinski-Powitz A. Expression of M-cadherin protein in myogenic cells during prenatal mouse development and differentiation of embryonic stem cells in culture. Dev. Dyn. 1994; 201:245–259. [PubMed: 7881128]

Ruiz-Gomez M, Coutts N, Price A, Taylor MV, Bate M. Drosophila dumbfounded: a myoblast attractant essential for fusion. Cell. 2000; 102:189–198. [PubMed: 10943839]

Rushton E, Drysdale R, Abmayr SM, Michelson AM, Bate M. Mutations in a novel gene, myoblast city, provide evidence in support of the founder cell hypothesis for Drosophila muscle development. Development. 1995; 121:1979–1988. [PubMed: 7635046]

Schroter RH, Lier S, Holz A, Bogdan S, Klambt C, Beck L, Renkawitz-Pohl R. kette and blown fuse interact genetically during the second fusion step of myogenesis in Drosophila. Development. 2004; 131:4501–4509. [PubMed: 15342475]

Shao X, Li C, Fernandez I, Zhang X, Sudhof TC, Rizo J. Synaptotagmin-syntaxin interaction: the C2 domain as a Ca2+-dependent electrostatic switch. Neuron. 1997; 18:133–142. [PubMed: 9010211]

Snow MH. Myogenic cell formation in regenerating rat skeletal muscle injured by mincing. II. An autoradiographic study. Anat. Rec. 1977; 188:201–217. [PubMed: 869238]

Strunkelnberg M, Bonengel B, Moda LM, Hertenstein A, de Couet HG, Ramos RG, Fischbach KF. rst and its paralogue kirre act redundantly during embryonic muscle development in Drosophila. Development. 2001; 128:4229–4239. [PubMed: 11684659]

Yaffe D, Saxel O. Serial passaging and differentiation of myogenic cells isolated from dystrophic mouse muscle. Nature. 1977; 270:725–727. [PubMed: 563524]

Zeschnigk M, Kozian D, Kuch C, Schmoll M, Starzinski-Powitz A. Involvement of M-cadherin in terminal differentiation of skeletal muscle cells. J. Cell Sci. 1995; 108:2973–2981. [PubMed: 8537437]

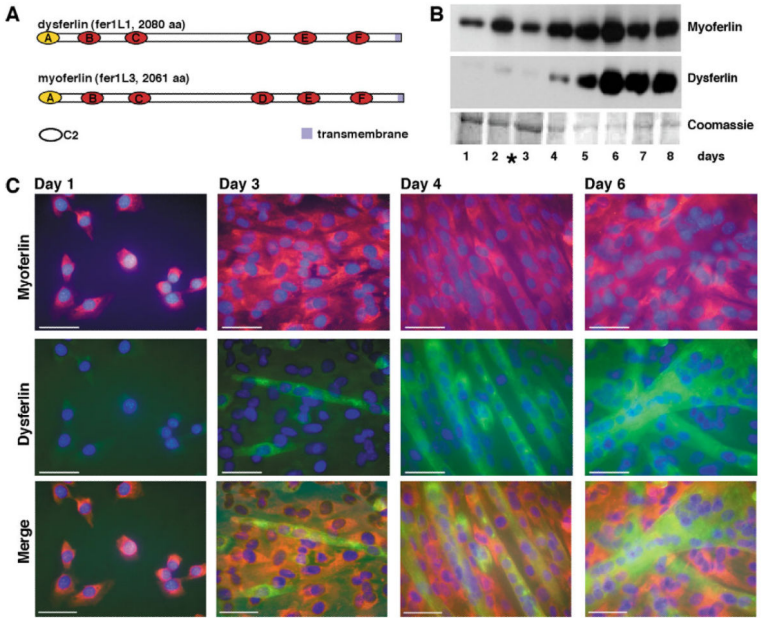

Figure 1.

Ferlin protein expression during muscle development. (A) Myoferlin and dysferlin are 230 kDa transmembrane proteins in the ferlin family. Their amino acid sequences are 74% similar and contain six cytoplasmic C2 domains. Myoferlin and dysferlin are expressed in skeletal muscle and in the muscle cell line C2C12. (B) During C2C12 cell differentiation, immunoblotting showed that myoferlin was expressed earlier in differentiation than was dysferlin. The asterisk indicates the switch from growth to differentiation media. These timepoints represent cultures containing a mixture of myoblasts and myotubes. (C) Images taken during C2C12 differentiation, corresponding to the timepoints shown in B. Scale bar: 50 μm. The same cell cultures were co-stained for myoferlin (red) and dysferlin (green). Myoferlin was expressed earlier and was expressed highly in singly nucleated myoblasts. Dysferlin expression was detected only in multinucleated myotubes.

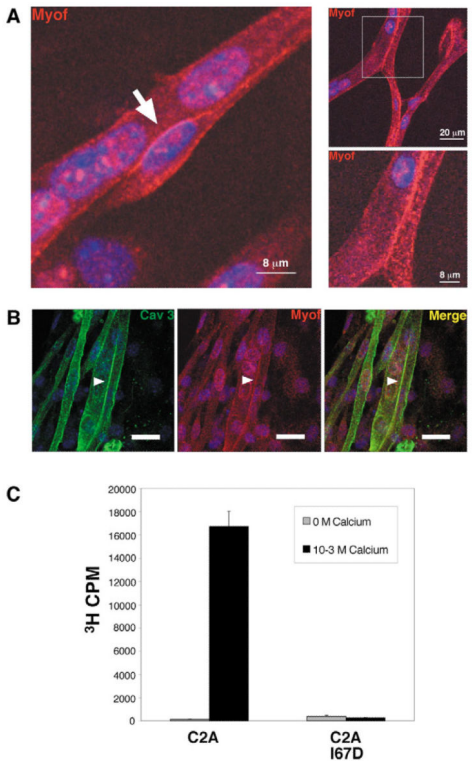

Figure 2.

Myoferlin is concentrated at sites of membrane fusion. (A) Confocal images of differentiating myoblasts, where myoferlin (red) appeared at the membrane, concentrated at sites of cell-cell contact (arrow and boxed area). (B) Regions of enhanced myoferlin immunoreactivity (red; and arrowhead) corresponded with membrane, as they were also positive for caveolin 3 immunoreactivity (green; arrowhead). Scale bar: 20 μm. (C) The C2A domain of myoferlin was generated as a GST-fusion protein and tested for calcium-sensitive lipid binding to ^{3}H-labeled vesicles containing 50% phosphotidylcholine and 50% phosphotidylserine. Binding to C2A required the presence of calcium. Myoferlin C2A engineered with the mutation I67D showed no phospholipid binding in the presence of calcium. This mutation is predicted to disrupt the hydrophobic packing of the β-strands of the myoferlin C2A domain.

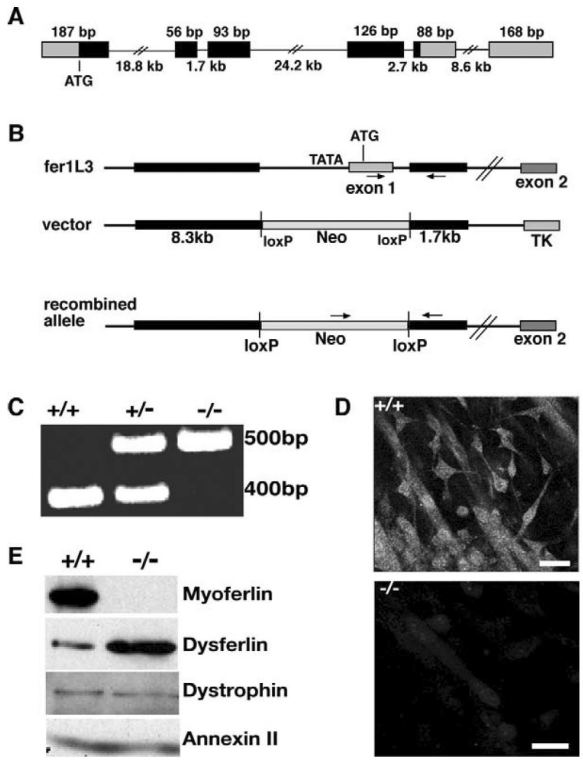

Figure 3.

Targeted homologous disruption of the murine myoferlin (*fer1L3*) locus. (A) Gene structure of the first six exons of myoferlin, showing the start codon (ATG). Those regions that encode the C2A domain are shown in black. (B) A neomycin-containing cassette was used to replace the transcriptional and translational start site of myoferlin. The thick black bars represent the homology arms present in the targeting construct. (C) PCR confirmed the replacement of exon 1 with neomycin. (D) Immunofluorescence microscopy using the MYOF3 antibody reveals that myoferlin null myoblasts do not express myoferlin protein. Scale bar: 20 μm. (E) Partially differentiated cultures of primary myoblasts from myoferlin null mice expressed no myoferlin protein, as detected by immunoblotting with an anti-myoferlin antibody whose epitope does not reside in the deleted region. An increased level of dysferlin expression was noted, while levels of other membrane associated proteins, dystrophin and annexin II, were unchanged.

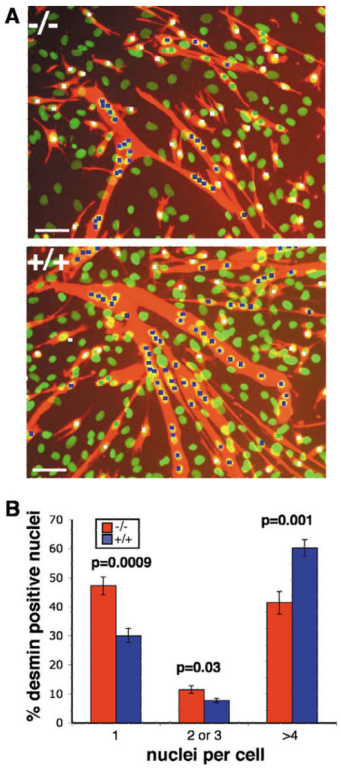

Figure 4.

Myoferlin null myoblasts show impaired fusion in vitro. (A) Myoblasts isolated from littermate control and myoferlin null neonatal mice were plated at equal densities and induced to differentiate. After 4 days of differentiation, cells were fixed and stained with anti-desmin antibodies (red) and Sytox nuclear dye (green). Scale bar: 50 μm. (B) Desmin is expressed only in myogenic cells, so the efficiency of fusion was determined by quantifying the number of singly nucleated desmin-positive cells (white squares), those containing two to three (green squares) nuclei, and those containing four or more nuclei (blue squares). The percentage of nuclei not associated with desmin staining was equivalent in wild-type and myoferlin null cultures, and these nuclei were not included when determining fusion efficiency. Myoferlin null cultures displayed significantly more desmin-positive single nuclei than did littermate control cultures. Myotubes containing four or more nuclei were reduced in myoferlin null cultures. Eight 10× fields from each genotype were used for quantification, comprising 2390 wild-type and 2485 myoferlin null nuclei.

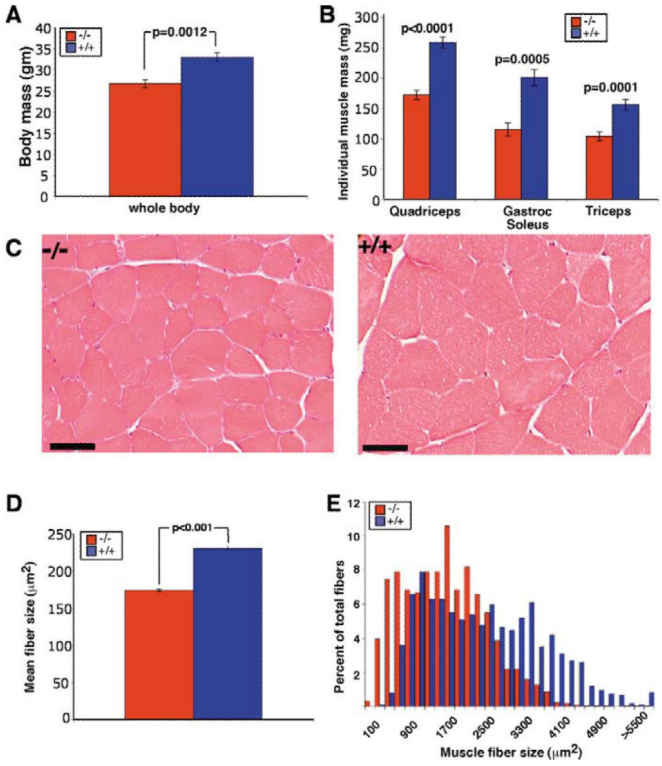

Figure 5.

Myoferlin null mice have a decreased body mass and muscle mass, and the muscle fibers of myoferlin null animals are decreased in area and size. Individual muscles were dissected, weighed and preserved for histology. (A) Body mass was significantly less in myoferlin null mice than in littermate control mice. (B) Individual muscle mass was also reduced in myoferlin null mice compared with in littermate controls. (C) Representative cross-sections of myoferlin null and wild-type quadriceps muscle. Scale bar: 50 μm. Multiple images of cross-sections through the belly of the quadriceps were used to quantify fiber size, revealing that the average area of myoferlin null fibers is reduced. (D) The mean wild-type fiber size was 2301 μm^2 whereas the myoferlin null mean was 1740 μm^2. (E) The distribution of fiber sizes was also examined and showed that myoferlin null muscle is composed of smaller fibers, and specifically lacks the largest fibers. 1740 wildtype and 2240 myoferlin null fibers were measured from 21 images of each genotype.

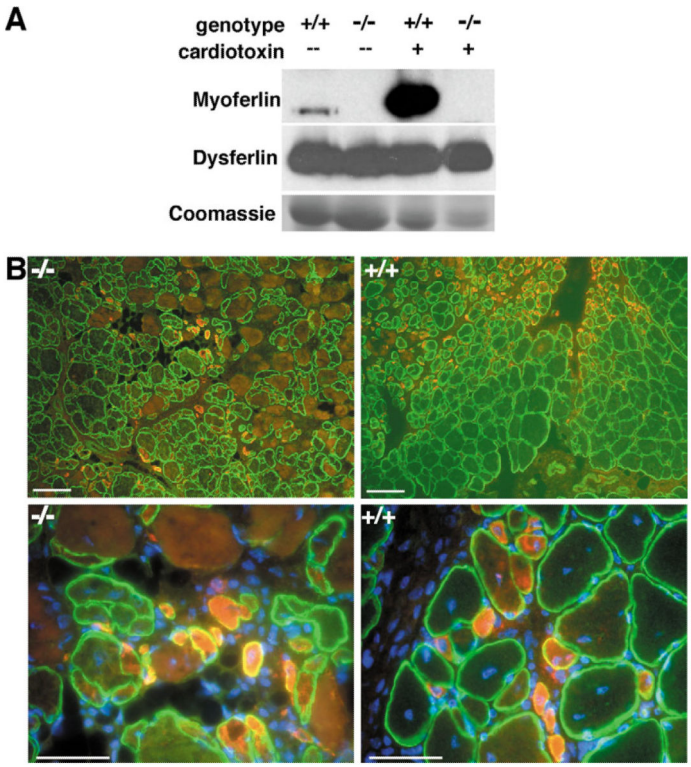

Figure 6.

Myoferlin is highly upregulated after muscle injury. (A) Immunoblot of muscle extracts 5 days after cardiotoxin injection showing marked upregulation of myoferlin after injury. Dysferlin was not upregulated after cardiotoxin-induced injury in either myoferlin null or wild-type mice. (B) Myoferlin null muscle does not regain its normal architecture after cardiotoxin injection. At low magnification (scale bar: 100 μm), dystrophin staining (green) shows smaller, more irregular fibers in myoferlin null muscle than in wild-type muscle. Embryonic myosin heavy chain (red) indicates regenerating myofibers. Higher magnification images (scale bar: 50 μm) show an increase in the number of centrally placed nuclei, which is indicative of recent fusion, in wild type compared with in myoferlin null muscle. Nuclei are stained with DAPI (blue).

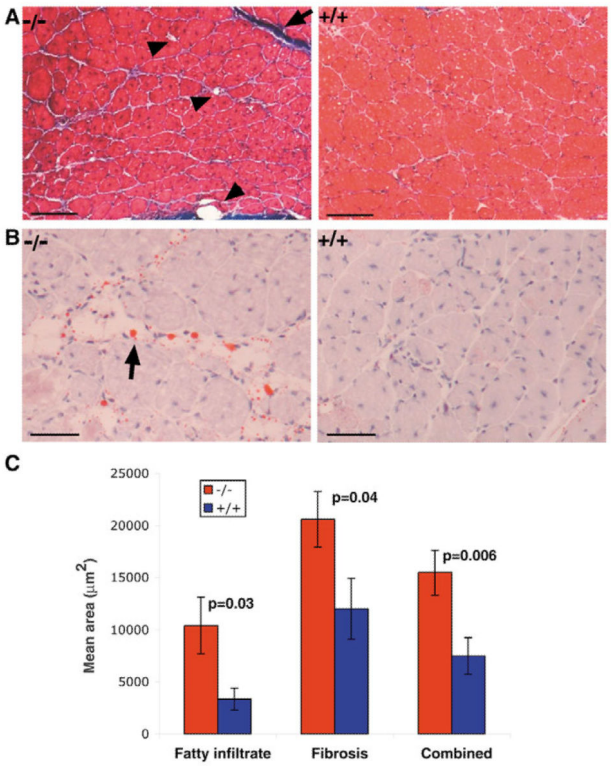

Figure 7.

Myoferlin null muscle regenerates less effectively and shows more fibrofatty infiltrate than does littermate control muscle after cardiotoxin injection. (A) In Mason Trichrome-stained sections of gastrocnemius muscles 9 days after cardiotoxin injection, fatty infiltrates appear white (arrowheads) and fibrotic tissue appears blue (arrows). Scale bar: 100 μm. (B) In sections stained with Oil Red O and Hematoxylin counterstain 13 days after injection, areas of fatty infiltrate appear as round white cells with orange droplets in the myoferlin null tissue. Scale bar: 50 μm. (C) ImageJ was used to quantify the area covered by fatty infiltrates and fibrotic tissue in four images of Trichrome-stained tissue, such as those shown in A, at each of three time points, days 9, 11 and 13 post-injection. Significantly more muscle was replaced with fibrofatty tissue in myoferlin null mice than in wild type.